Planetary and Space Science 66 (2012) 71–78

Contents lists available at SciVerse ScienceDirect

Planetary and Space Science

journal homepage: www.elsevier.com/locate/pss

Boulders on Lutetia

Michael Küppers [a,*], Richard Moissl [a], Jean-Baptiste Vincent [b], Sébastien Besse [c], Stubbe F. Hviid [b], Benoît Carry [a], Björn Grieger [a], Holger Sierks [b], Horst Uwe Keller [d], Simone Marchi [e], the OSIRIS team[1]

[a] European Space Agency-European Space Astronomy Centre, PO Box 78, 28691 Villanueva de la Cañada, Spain
[b] Max-Planck-Institut für Sonnensystemforschung, Max-Planck-Str. 2, 37191 Katlenburg-Lindau, Germany
[c] Department for Astronomy, University of Maryland, College Park, MD 20742-2421, USA
[d] Institute for Geophysics and Extraterrestrial Physics, TU Braunschweig, 38106 Braunschweig, Germany
[e] Universite de Nice-Sophia Antipolis, Observatoire de la Cote d'Azur, CNRS, 06304 Nice, France

ARTICLE INFO

Article history:
Received 22 June 2011
Received in revised form
3 November 2011
Accepted 7 November 2011
Available online 25 November 2011

Keywords:
Lutetia
Boulders
Cratering
Imaging

ABSTRACT

More than 200 boulders are among the many prominent geological features seen on Lutetia by the OSIRIS cameras onboard Rosetta. Most are concentrated around the central crater in Baetica regio with a few more apparently associated with Patavium crater. The size range of boulders visible to OSIRIS is about 60–300 m. We model the trajectories of boulders ejected from the central crater and show that their distribution is consistent with most of them being created from that crater, similar to the situation on asteroid Eros where most of the boulders are believed to originate from Shoemaker crater. We evaluate various destruction mechanisms for ejecta blocks and conclude that, using current estimates of the number of small asteroids in the main belt, destruction by impacts of small (several meters diameter) projectiles limits the lifetime of the boulders (and the age of the central crater) to a maximum of 300 million years. Since several analyses of crater ages and size distributions also come up with surprisingly young ages, the size-frequency distribution of small main-belt asteroids (below the size currently reached by surveys) may warrant to be revisited.

1. Introduction

During the Rosetta flyby of asteroid (21) Lutetia, about 50% of the surface of the asteroid was imaged with high resolution (up to 60 m/pixel) by the OSIRIS Narrow Angle Camera [NAC] (Sierks et al., 2011). Lutetia is exceptionally rich in its geomorphological history (Thomas et al., 2012). Among the many features identified, a large number of boulders show up prominently as positive relief features, typically close to the resolution limit, with shadows next to them, important for their identification.

Fig. 1 shows that most of the boulders are concentrated around the central crater cluster in Baetica, with some more visible close to Patavium crater, at the border between Noricum and Narbonensis (see Thomas et al., 2012; Massironi et al., 2012 for the definition of the regions on Lutetia). The highly irregular spatial distribution close to big craters suggests connection of the boulders with the creation of those individual craters. Indeed, for asteroid (433) Eros it is has been postulated that most of the boulders there originated from a single large impact crater (Thomas et al., 2001).

The association of boulders with individual craters implies information about the history of the asteroid. The "boulder forming" impacts are most likely the youngest of their size range. Estimates of the lifetime of boulders allow estimation of the age of the crater from which boulders were ejected.

In Section 2 we describe the identification methods of boulders and the resulting counts. We discuss the possible detection of secondary craters due to boulder impacts. Section 3 analyses the origin of the boulders and derives age constraints for large craters on Lutetia. Concluding remarks are given in Section 4.

2. Boulder identification and counts

In order to measure a size distribution for the boulders visible on the surface of Lutetia we first define the type of feature we will identify and count as boulders. This is especially important at the resolution limit at which it becomes difficult to distinguish boulders from other features such as small craters of the same dimensions, which appear very similar in the OSIRIS images.

* Corresponding author. Tel.: +34 91 8131 149; fax: +34 91 8131 325.
E-mail address: michael.kueppers@sciops.esa.int (M. Küppers).

[1] M. A'Hearn, F. Angrilli, C. Barbieri, A. Barucci, J.-L. Bertaux, G. Cremonese, V. Da Deppo, B. Davidsson, S. Debei, M. De Cecco, S. Fornasier, M. Fulle, O. Groussin, P. Gutiérrez, W.-H. Ip, L. Jorda, D. Koschny, J. Knollenberg, J. R Kramm, E. Kührt, P. Lamy, L. M. Lara, M. Lazzarin, J. J. López-Moreno, F. Marzari, H. Michalik, G. Naletto, H. Rickman, R. Rodrigo, L. Sabau, N. Thomas, K.-P. Wenzel.

0032-0633/$ - see front matter © 2011 Elsevier Ltd. All rights reserved.
doi:10.1016/j.pss.2011.11.004

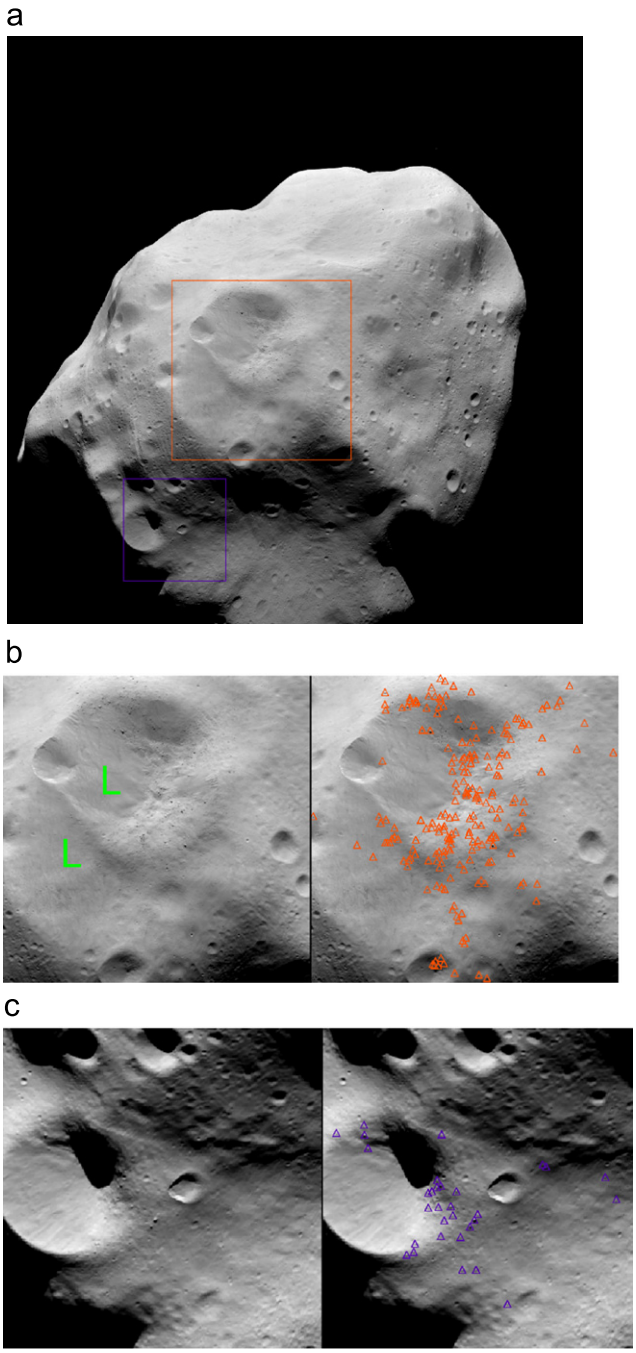

Fig. 1. (a) Overview image. The red (image centre) and blue (towards bottom left) boxes indicate the regions shown in b and c, respectively. All boulders found on Lutetia are within those regions. (b) Central crater in Baetica region. "L" on the left image indicates a landslide. All boulders found in the region are indicate on the image to the right. (c) Region near Patavium crater. All boulders found in this region are indicated in the image to the right. (For interpretation of the references to color in this figure legend, the reader is referred to the web version of this article.).

The chosen identification criteria were:

- clearly identifiable brightness variation (from above to below average value).
- "Convex feature": a bright positive relief feature must be seen with a dark one (its shadow) next to it. The direction of the shadow must be consistent with the position of the sun.

As the resolution is limited to ~60 m/pixel in the OSIRIS images around closest approach, the features identified as boulders according to the above criteria could still contain unresolved sub-structure. As a result of the point spread function (PSF) of ~1.6 pixels, only the largest ones of them ($\geq$200 m in diameter) are clearly visible as single entities. The smaller identified boulders only fulfill the requirements set for classification as convex features. Therefore some features might actually be either localized accumulations of smaller material (mounds) or rocky outcrops (e.g., on the slopes of the central crater). During the measurements there were also a number of small craters, of similar dimensions as the boulders detected in close vicinity to the measured features (Fig. 2). This is a potential indication of secondary craters associated with the boulder creation mechanism (e.g. from boulders, which impacted in a loose layer of regolith).

We selected the following images for the boulder count:

*NAC*_2010−07−10*T*15.42.47.523*Z_IS*40_1251276001_*F*22.*img* (scale = 67.0 *m*/px) and

*NAC*_2010−07−10*T*15.44.48.158*Z_IS*40_1251276000_*F*22.*img* (scale = 59.7 *m*/px)

They were chosen because they show most of the illuminated northern hemisphere of Lutetia and were among the highest resolution images. Both images were taken with the "orange" filter centered at 649 nm with a bandwidth of 85 nm full width half maximum.

The analysis starts with calibrated and distortion corrected images (Level 3). The images have been sharpened by deconvolution with the point spread function of the camera and displayed with a factor of two, non-interpolated, magnification and maximized contrast. Boulders were identified by visual inspection.

For each identified feature two positions (P1, P2) have been recorded, separated by the largest elongation of the feature. The boulder positions and diameters follow therefore as the middle point between the two measured positions and the separation in distance. For future reference we recorded a version of each evaluated image with the identified boulder positions (see Fig. 1).

We evaluated the resulting size distribution to an accuracy of one image pixel, which represents the estimated measurement accuracy. Although, owing to the presence of shadows, the identification of objects is not limited to the camera resolution of 2 pixels, we estimate the count to be incomplete for boulders of smaller sizes (below 120 m). This corresponds to a completeness limit at a total feature size (boulder+shadow) of about 4 pixels, comparable to that typical of crater counts (e.g., Marchi et al., 2010).

We identified 203 boulders close to the central crater and 31 more in and around Patavium crater. No boulders are seen on the landslides of the central crater. Since the landslides may have buried boulders, there is no evidence for an asymmetry in the direction of boulder ejection. The size distribution of the boulders in the central crater is shown in Figs. 3 and 4.

3. Origin and evolution

Here we first investigate the hypothesis that most of the boulders were ejected from 2 individual craters. We compare boulder sizes and spatial distributions with those expected from impacts into hard rock. We then analyze the presence and size distribution of the boulders in terms of the age of the producing craters. In our analysis we concentrate on the central crater that provides best statistics.

3.1. Boulder size distribution

The empirical size distribution of the boulders was determined in Sect. 2. Here we compare it to theoretical distributions, assuming that most of the boulders were created from two

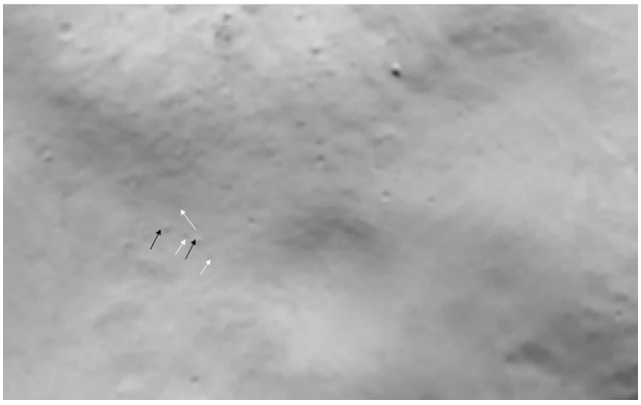

Fig. 2. Boulders close to similarly sized craters. The white and black arrows denote craters and boulders, respectively. While it is difficult to clearly identify boulders with individual (secondary) craters, there is a clear correlation between boulder density and crater density, suggesting that some craters may be secondaries created from impact by boulders.

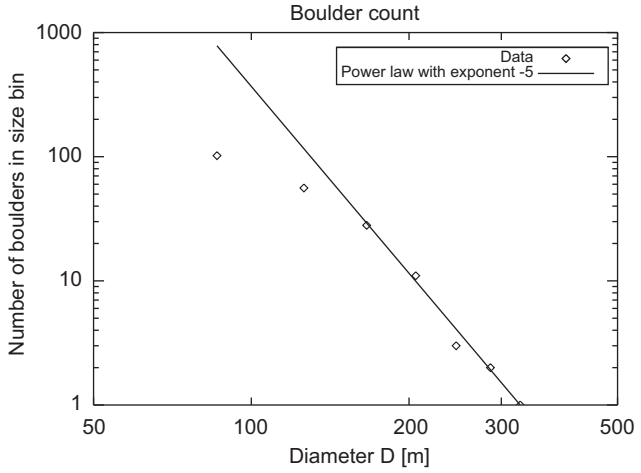

Fig. 3. Measured size distribution of boulders on Lutetia. The count may be incomplete for the two smallest size bins. Overplotted is a power law distribution with an exponent of −5. The bin size is 40 m.

individual impacts into rock. The large size of the boulders requires impact into rock (as opposed to impact into regolith) as their formation mechanism. This is also consistent with the crater being much deeper than the estimated regolith depth on Lutetia (a few km crater depth vs. a few hundred meter regolith depth, Vincent et al., 2012).

O'Keefe and Ahrens (1987) used empirical data over a wide range of scales to derive the size-velocity distribution of impact ejecta. In particular, for impact and explosion events, the mass of the largest ejecta fragment M_L is related to the total mass of ejecta M_T by a power law:

$$M_L = 0.05 M_T^{0.8}, \quad (1)$$

Where, masses are in kg. The relation is based on data for ejecta masses between about 1 kg and $>10^{14}$ kg. If we approximate the central crater as a spherical cap, its mass is

$$M_T = r^3\pi(1/(2a)+1/(6a^3))\rho \quad (2)$$

Here $r=10.5$ km is the crater radius, $a=2.5$ the radius/depth ratio (Vincent et al., 2012), and $\rho=3400$ kg/m^3 (Sierks et al., 2011) the bulk density of Lutetia. With the resulting ejecta mass of $\sim 10^{15}$ kg, the mass of the largest fragment is 5.7×10^{10} kg and its size (taken as $(M_L/\rho)^{1/3}$) is 310 m, in agreement with the size of the largest fragments found.

Instead of Eq. (1), several authors (e.g., Lee et al., 1996) used $D_L=0.25\ d^{0.7}$ for the size of the largest fragment (with d the crater diameter). The relation is based on a study of lunar craters. Generally, the predictions of both scaling laws are similar. For the central crater on Lutetia, the size expected from the relation from Lee et al. would be 265 m, in the same range as found with Eq. (1). Most of the discrepancy Lee et al. find when comparing the predictions of Eq. (1) with their scaling law for the size of the largest boulder on (243) Ida is caused by their incorrect conversion of Eq. (1) from grams to kg. Both scaling laws also predict the correct range for the largest boulder on Eros (150 m, Thomas et al., 2001), assuming Shoemaker crater as the source.

The size distribution of the boulders near the central crater cluster is shown in Fig. 3. The largest boulders show a differential size distribution that follows a power law index of about −5, comparable to results for Eros (Thomas et al., 2001; Chapman et al., 2002), but steeper than for Itokawa (Michikama et al.,

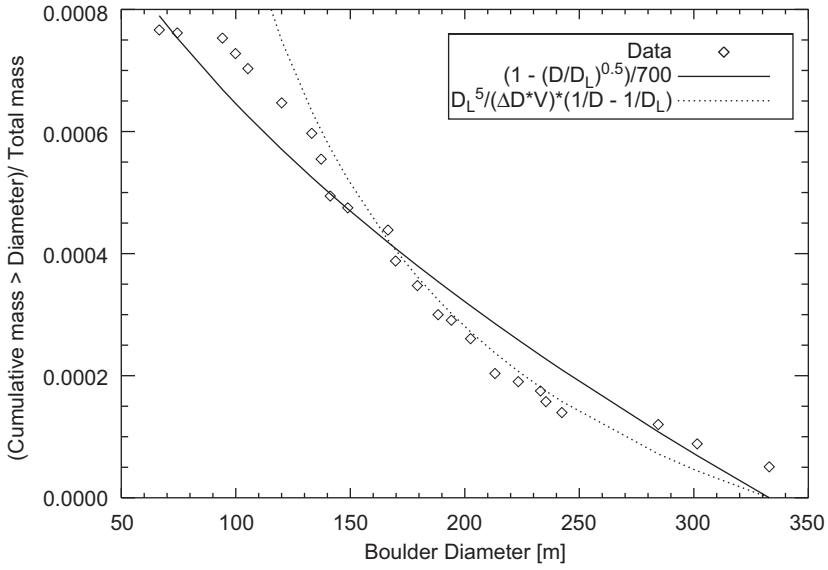

Fig. 4. Cumulative size distribution of boulders. The count may be incomplete for sizes <120 m. The solid line is the size distribution according to Eq. (3), divided by 700 (i.e., Eq. (3) predicts nearly 3 orders of magnitude too many boulders), the dashed line is the distribution according to Eq. (4), corresponding to the differential size distribution shown in Fig. 3.

2008). The boulders on Itokawa were most likely created by the catastrophic impact that formed the asteroid (Fujiwara et al., 2006). The shallower size distribution of its boulders may mean that it is collisionally younger (has suffered fewer impacts) than Shoemaker crater on Eros and the central crater on Lutetia. That would mean that Itokawa spent less time in the main belt than Eros did after creation of Shoemaker crater or Lutetia did after creation of the central crater. Alternatively, smaller ejecta blocks may have been preferentially removed during the impact that formed Itokawa.

For boulder size smaller than about 150 m, the size distribution becomes shallower. A similar change in slope was observed for Eros (Thomas et al., 2001). It may indicate more efficient destruction of larger blocks or, in the case of Lutetia, incompleteness of the boulder count for smaller blocks.

The cumulative mass distribution from experimental craters or explosion events typically follows a power law with a slope of 0.5 (Hörz and Cintala, 1997). However, the biggest ejecta blocks of large craters on the Moon, Mars or Eros contain a much smaller fraction of the total ejected mass than expected from the law:

$$M_C/M_T = 1-(D/D_L)^{0.5} \tag{3}$$

with the mass M_C of all fragments with diameter larger than D and D_L the diameter of the largest ejecta block (e.g., Cintala et al., 1982).

Fig. 4 shows that the same discrepancy exists for Lutetia: Eq. (3) predicts approximately 700 times more boulders than are observed. While it largely overestimates the total number of boulders, it is a reasonable approximation to the relative size distribution. Also shown in Fig. 4 is the cumulative mass distribution expected from the power law size distribution shown in Fig. 3:

$$M_C/M_T = 1/M_T \int_D^{D_L} N(D')M(D')dD' = \frac{1}{\rho V}\int_D^{D_L}\left(\frac{D'}{D_L}\right)^{-5}\frac{1}{\Delta D}D'^3\rho dD' = \frac{D_L^5}{V\Delta D}\left(\frac{1}{D}-\frac{1}{D_L}\right) \tag{4}$$

Here $N(D)$ is the differential size distribution, $V=M_T/\rho$ the crater volume taken from Eq. (2), and $\Delta D=40$ m the size bin, chosen as the approximate size difference of the largest boulders. Eq. (4) shows that if the differential size distribution is a power law, then the cumulative distribution approximates a power law only for $D \ll D_L$. In other words, Eq. (3) is invalid for the largest ejecta.

3.2. Boulder ejection velocities and spatial distribution

Lutetia is the first case where most of the boulders on an asteroid appear clearly connected to individual craters (Fig. 1). While Shoemaker crater is most likely the source of most boulders on Eros (Thomas et al., 2001), due to the smaller size of that asteroid the distribution is more global. The situation on Lutetia may be best compared to Phobos were most large ejecta blocks that are close to or inside Stickney crater (Thomas, 1979).

Here we test if the concentration of impact ejecta blocks around the central crater is indeed expected for Lutetia. We model the trajectories of boulders ejected from the central crater. Each boulder is launched from a random location within the crater. The direction of ejection is outward from the center of the crater with an angle of 40° relative to the local surface (following Housen et al., 1983 and references therein).

The choice of the ejection speed for the model follows the derivation for the mass-velocity distribution of impact ejecta from O'Keefe and Ahrens (1987). It uses Eq. (1) and three other power laws: first, it is assumed that the mass M_{Lv} of the largest fragment ejected at a given velocity v is described by:

$$M_{Lv}/M_L = (v/v_{min})^{-\delta} \tag{5}$$

Here M_L is the mass of the largest fragment and v_{min} the minimum ejecta velocity. The exponent $\delta \sim 4$ for rock is derived from a combination of the theory of fracture of rocks (Grady and Kipp, 1980) and crater ejecta scaling theory (Housen et al., 1983). Second, the total mass M_a of fragments are larger than mass M ejected at a given velocity is:

$$M_a = m_v(1-(M/M_{Lv})^{\beta/3}) \tag{6}$$

with the total mass m_v of all fragments ejected between velocity v and $v+dv$ and $\beta=0.5$ the same exponent in the size distribution of ejecta fragments as used in Eq. (3) (but here for ejecta of a given velocity). The third power law holds for the velocity distribution of fragments:

$$m_v = (\xi M_T/v_{min})(v/v_{min})^{-(\xi+1)} \tag{7}$$

Here the exponent ξ can be determined from scaling theory or experiment and is about 1.5 for rock. Finally, the mass of fragments ejected at a velocity higher than v and with a mass larger than M is given by:

$$M_{mv} = \int_v^{v_{max}} M_a(v')dv', \tag{8}$$

where v_{max} is determined by the condition M_{Lv} $(v_{max})=M$ in Eq. (5) and the integral is evaluated using Eqs. (6) and (7). The final result is:

$$M_{mv} = M_T((v/v_{min})^{-\xi}-(M/M_L)^{\xi/\delta} + \xi/(\delta\beta/3-\xi))((v/v_{min})^{\delta\beta/3-\xi}(M/M_L)^{\beta/3}-(M/M_L)^{\xi/\delta})) \tag{9}$$

The minimum ejection velocity v_{min} was derived from the crater ejection scaling laws from Housen et al. (1983):

$$v = (K_1\sqrt{gr}+K_2\sqrt{Y/\rho})(x/r)^{-1/\mu} \tag{10}$$

Impact scaling theory distinguishes between strength-dominated cratering with the crater size limited by the strength of the target material and gravity-dominated cratering with crater size limited by target gravity (e.g., Holsapple, 1993). Since the impact that created the central crater on Lutetia is somewhere in the transition between the two regimes, we used the sum of the expressions for the 2 cases. The constants $K_1=0.62$ and $K_2=0.1$ were taken from Housen et al. (1983), the average gravity g of Lutetia is 0.0473 m/s^2 (taken as that of the equivalent sphere of 49 km radius and density of 3400 kg/m^3, Sierks et al. (2011)), and the "impact strength" of the target was taken as 2.5×10^6 Pa, a typical value for rock at about 100 m scales (Holsapple, 1993). The target strength is the least constrained parameter in Eq. (10), but v_{min} is relatively insensitive to it. For $Y=2.5\times10^6$ Pa the minimum velocity is 16.5 m/s, for $Y=0$ it would be $v_{min}=13.8$ m/s, while increasing Y by an order of magnitude to 2.5×10^7 Pa would result in $v_{min}=22.4$ m/s.

The minimum velocity in Eq. (10) is for ejecta launched at the crater edge (distance x from crater center reaches the crater radius r). This derivation somewhat overestimates v_{min} because the scaling law in Eq. (10) breaks down close to the crater rim (e.g., Housen and Holsapple, 2011). The consequence is that some very low velocity ejecta are not considered in the model (the number of boulders falling into the crater may be underestimated). However, most ejecta are still described correctly and the general distribution of ejecta on the asteroid is not affected by the limit of the validity of the scaling law.

For each boulder we eject in the model, Eq. (9) is used to get the launch velocity. Since the minimum size of boulders we can detect is about 60 m or about 1/5 of the diameter of the largest one, we only consider ejecta with a minimum mass M_{min} so that

$M_{min}/M_L = 1/125$. A random number between 0 and 1 is drawn and the velocity v is chosen so that the random number represents M_{mv} (v, M_{min})/M_{mv} (v_{min}, M_{min}) (the fraction of boulders heavier than M_{min} that are ejected faster than v).

The ballistic trajectory of the boulders is then integrated in the gravity field of the asteroid. The shape model presented in Sierks et al. (2011) is used to compute the acceleration due to gravity at each time step using the analytical formula for the gravity of a homogeneous polyhedron (Werner, 1994). Calculations are done in the body-fixed frame, taking into account centrifugal force and coriolis force with the rotation period of the asteroid of 8.16827 h (Carry et al., 2010). A time step of 1 s was used for the calculations. The program was validated by comparing trajectories of sample particles with the trajectory propagator roviz (Grieger et al., 2011). The results for the landing point agree to within 150 m.

The result of a run with 500 boulders is shown in Fig. 5. Most boulders land within 5–10 km from the crater rim, in agreement with their observed distribution in Fig. 1. Azimuthally the distribution appears roughly isotropic, so the lack of boulders in the landslide suggests that the landslide buried many boulders, implying a depth of the slid material of 100–200 m. The boulders traveling further away from the crater are not concentrated in the Noricum and Narbonensis regions, so the ejecta blocks seen there are from another impact, most likely Patavium crater as indicated in Fig. 1.

3.3. Boulder destruction mechanisms and age

Boulders are not uniformly distributed but concentrated around large craters. This implies that the presence of boulders constrains the age of big impact structures. Here we use the lifetime of boulders against various destruction mechanisms to estimate the age of the central crater on Lutetia.

3.3.1. Destruction by impact

Boulders may be destroyed when being hit by later impactors. Lutetia, or at least its outer few tens of kms, are made of rocky material, with the specific composition still being under debate (e.g., Vernazza et al., 2009; Belskaya et al., 2010). Therefore we use general results for rocky objects to estimate the size of an impactor needed to disrupt a boulder on Lutetia. From the results of the smooth particle hydrodynamics simulations by Benz and Asphaug (1999), a specific energy of $Q^*=470$ J/kg is needed to catastrophically disrupt a basalt target of 100 m size at an impact velocity of 5 km/s, a typical relative velocity in the asteroid main belt Bottke et al. (2005a) arrives at a similar result for the catastrophic disruptions of asteroids from a model of the collisional evolution of the asteroid belt. The corresponding minimum size of an impactor that disrupts a boulder on Lutetia is determined from:

$$Q^* = \tfrac{1}{2} M_i v_i^2 / M_B = \tfrac{1}{2} \rho_i d_i^3 v_i^2 / (\rho_B d_B^3) \quad (11)$$

or

$$d_i = d_B (Q^* \rho_B / (\tfrac{1}{2} \rho_i v_i^2))^{1/3} \quad (12)$$

Here M is the mass, d the diameter, v the velocity, and ρ the density. The indices i and B refer to impactor and boulder, respectively. With $d_B=100$ m, $\rho_B=3400$ kg/m^3 (assumed to be the same as the bulk density of the asteroid), $\rho_i=2000$ kg/m^3, and $v_i=5$ km/s, a minimum impactor size of about 4 m is needed to disrupt a boulder of 100 m diameter.

There are of the order of 5×10^{11} asteroids >4 m in the main belt and the collision probability between them is of order $P=2.5 \times 10^{-18}$ km^{-2} yr^{-1} (Bottke et al., 2005b). Consequently, an ejecta block with a surface of 100 m $\times$ 100 m would be catastrophically hit every 80 million years. This is consistent with Bottke et al.'s statement that the collisional lifetime of a 100 m asteroid is 64 million years. If we take input values determined for Lutetia by Marchi et al. (2012) instead ($v=4.3$ km/s and $P=4.1 \times 10^{-18}$ km^{-2} yr^{-1}), the lifetime is only about 50 million years. Those numbers need to be increased by approximately a factor of 2 (to a lifetime of 100–160 million) to correct for the fact that the boulder can be impacted from 2π sterad only (as opposed to 4π for an asteroid). Allowing in addition for some comminution of the original boulder population created by the impact, the upper limit for the age of the central crater is about 300 million years.

Impacts that create craters larger than a boulder may destroy ejecta blocks even if they do not hit them. If the boulder is within the crater, it may be disrupted. In that case the crater radius may be the relevant size scale, not the size of the boulder. Then the lifetime t_B of a boulder is given by:

$$t_B = \frac{1}{P/2 \int_{4\,\mathrm{m}}^{3000\,\mathrm{m}} N(D) \max((r_c(D))^2 \pi, 0.01\,\mathrm{km}^2) dD} \quad (13)$$

with the differential size distribution $N(D)$ (in 1/m), the crater radius r_c created by the impact of a boulder with diameter D, and 0.01 km^2 the surface area of a 100 m boulder. The impact probability P is divided by 2 to account for the limited solid angle "seen" by a boulder.

The evaluation requires the differential size distribution of impactors on Lutetia between 4 m (the smallest projectile that destroys a typical boulder) and 3 km (no other large craters than the central crater are seen close to the locations of the boulder fields). For the larger end of this size range (down to about 0.5 km diameter) the differential size-frequency distribution of main-belt asteroids is constrained to a power law with an index between 2.3 and 2.5 (Yoshida and Nakamura, 2007; Gladman et al, 2009). For smaller objects, near-earth asteroids show a change towards a steeper slope of 3.5 of the size-frequency distribution for diameters smaller than about 300 m (slightly steeper than that determined in Stokes et al., 2003, see Bottke et al., 2005b and references therein for a compilation of observational data).

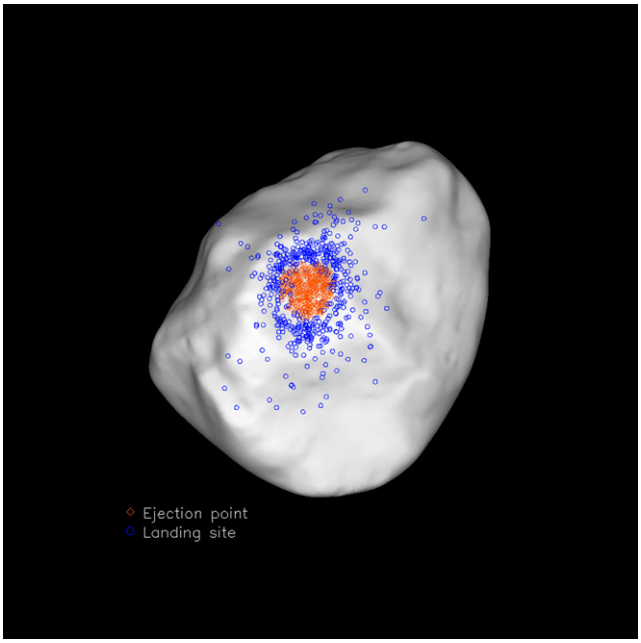

Fig. 5. Modeled trajectories of 500 boulders. The red points are the positions of ejections, the blue points the landing positions of the boulders.a. (For interpretation of the references to color in this figure legend, the reader is referred to the web version of this article.).

This slope is consistent with the model of Bottke et al., 2005b for the size distribution of main-belt asteroids. Therefore we take the following size-frequency distribution for Asteroids that may impact Lutetia:

$$N(D) = 4 \times 10^{13} D^{-3.5} (D \leq 300\,\mathrm{m}) \\ = 7.5 \times 10^{10} D^{-2.4} (D > 300\,\mathrm{m}) \quad (14)$$

Here $N(D)$ is normalized so that the total numbers of objects >4 m is $5*10^{11}$.

Additionally, we determine the size r_c of a crater from a given impactor with radius r according to the scaling relationship from e.g., Holsapple (1993):

$$r_c = rC_1(3.22gr/v_I^2 + (C_2 Y/(\rho v_I^2))^{(2+\mu)/2})^{-\mu/(2+\mu)} \quad (15)$$

The constants are $C_1=0.86$ and $C_2=3$, the scaling exponent $\mu=0.55$, an impact velocity $v_I=5$ km/s was used and the other parameters were taken as in Eq. (10).

The resulting lifetime of a boulder estimated with Eq. (13) decreases to approximately 140 million years, only slightly below the lifetime of maximum 160 million years when considering the size of the boulder, not of the crater, as the limit for destruction. Realistically the destruction limit will be somewhere in between so we conclude that the maximum age of the central crater as derived from the ubiquitous presence of boulders is approximately 300 million years.

3.3.2. Burial of boulders by impact ejecta

Burial in large regolith layers created by impacts is another impact related mechanism that would not destroy boulders, but make them unobservable. We calculate the average regolith height created in a given time t similar to the destruction calculations in subsection 3.3.1:

$$h = V_R/A_L = Pt/4 \int N(D)V(D)dD' \quad (16)$$

Here V_R is the total regolith volume created in time t, A_L the surface area of Lutetia, and $V(D)$ the volume of the crater created from an impactor with diameter D (determined from Eqs. 15 and 2). The factor 4 is the ratio between surface area and cross section of Lutetia.

The regolith layer thickness depends critically on the size of the largest crater considered in Eq. (16). For a time span of 300 million years, the accumulated amount of regolith is about 210 m, comparable to the size of a boulder. Nevertheless burial by ejecta is unlikely to limit the "lifetime" of boulders. Most of the regolith is accumulated by a few large impacts. Reducing the maximum impactor size from 3 km to 1 km, the thickness of the regolith layer decreases to about 60 m, smaller than the observable boulders. Most of the regolith is created by rare, big impact events. From the images of the asteroid, it seems likely that the impact creating the central crater was the last big (impactor size a few kms) impact on the observed northern hemisphere of Lutetia. We cannot exclude the possibility of a recent large impact on the unobserved southern hemisphere. However, a run of the model presented in section 3.2.2 for the ejection velocity and emplacement of regolith in general (no lower mass limit) shows that on a big asteroid like Lutetia most of the regolith is distributed locally, relatively close to the crater. Even a statistically unlikely recent large impact on the southern hemisphere would not transport sufficient regolith to bury most of the north polar region where the central crater is located.

While burial by impact ejecta is unlikely to limit the lifetime of the boulders currently seen on Lutetia, rare large impact like the ones that created the big central crater and Massalia crater may erase previously existing boulders by burial and/or seismic shaking of the body. That may explain why all boulders we see can be associated with two individual craters.

3.3.3. Disintegration by thermal stress

Dombard et al. (2010) propose disaggregation by thermal stress as a destruction mechanism for the boulders on Eros. They suggest that the ponds visible on Eros are the remains of (partly) destroyed boulders. They show that ponds are seen preferable at low latitudes that experience more terminator crossings (and associated large temperature gradients) than polar regions (for both Eros and Lutetia the spin axis is close to the orbit plane).

Thermal stress is not expected to be an efficient destruction mechanism for the boulders observed close to the central crater on Lutetia. While the resolution of the flyby images is insufficient to check for the presence of ponds, the boulders ejected from the central crater are at high latitudes where terminator crossings are rare. Also, thermal gradients will be less extreme in the asteroid main belt than in near-earth space. As described by Dombard et al. (2010), even on Eros most boulders at high latitude are not associated with ponds. This does not exclude the possibility that the lifetime of boulders created at low latitude on Lutetia is effected by thermal stress.

4. Conclusions

Boulders are ubiquitous on small bodies. They were detected on Phobos and on all asteroids that have been imaged with sufficient spatial resolution from spacecraft. In many cases (Stickney on Phobos, Shoemaker crater on Eros, and the central crater on Lutetia presented here) they have been associated with large impact structures. We show that for Lutetia, gravity is strong enough that the concentration of ejecta blocks from impacts around the source crater is expected. In particular, applying scaling relationships for the size-velocity distribution of impact ejecta, boulders with sizes of several tens of meters or larger are not expected to escape Lutetia, consistent with the non-detection of a satellite by Bertini et al. (2012).

The size distribution of the boulders on Lutetia is steep. It is comparable to that on Eros, whereas that on Itokawa is somewhat shallower. Since boulders are the largest impact ejecta, comminution by later impacts will steepen their size distribution (the largest sizes will be destroyed, but not replenished). The differences seen between Itokawa on one hand and Eros and Lutetia on the other hand may reflect different processing stages on different asteroids, with the boulders on Itokawa having suffered less collisional modification.

Impacts of asteroids with a diameter of several meters is the dominant destruction mechanism for boulders on Lutetia. It limits their age and, by inference, that of the 20 km crater dominating the northern hemisphere, to a maximum of 300 million years. Given that the central crater is the second largest crater on the 50% of Lutetia imaged by OSIRIS and that Lutetia is most likely primordial (Sierks et al., 2011), the expected frequency of an impact creating a crater of 20 km or larger is about once per a billion years. It is notable that the age limit for the central crater on Lutetia would also apply to the impact that created the boulders seen by Galileo on Ida (Lee et al., 1996) and to the boulders ejected from Shoemaker crater on Eros (Thomas et al., 1991; in the case of Eros, 300 million years is the maximum time between the impact creating Shoemaker crater and the transfer of Eros from the main belt into near-earth space).

Furthermore, on asteroid Steins, visited by Rosetta in 2008 (Keller et al., 2010), a lack of craters below a diameter of 500–600 m was noted by Marchi et al. (2010). They explain the "missing" craters with a resurfacing event connected to the impact that formed Ruby crater, the largest crater on Steins. The corresponding age of Ruby

crater is inferred to be below 250 million years, compared to a collisional age of Steins of ~2.2 billion years. Quoting studies on Gaspra and Eros in addition to their investigation of the crater size-frequency distribution of Steins, Marchi et al. (2010) note that "Despite the low number statistics, the cratering age of the main belt asteroids smaller than ~20 km seems to be systematically younger than their collisional age."

Taken together, the large number of extraordinarily young craters derived from the presence of boulders and from crater size distributions is unlikely to be a statistical fluke. Therefore a critical review of the input data of the age determination is due. The age or lifetime calculations depend on two quantities: firstly the scaling relations used to determine the catastrophic disruption threshold for ejecta blocks or crater size vs. impactor size, and secondly the size-frequency distribution of asteroids in the main belt.

Crater scaling relationships are well established (e.g., Holsapple and Housen, 2007) and asteroid evolution models now derive scaling laws for the catastrophic disruption threshold that agree with those from hydrocode models (Bottke et al., 2005a). Therefore in the following we discuss the possibility that the number of small main-belt asteroids maybe overestimated.

The size-frequency distribution of main-belt asteroids in Bottke et al. (2005b) is the output of a model of the collisional and dynamical evolution of the asteroid belt. The resulting size distribution fits the observed distribution for main-belt asteroids >1 km, and for near-earth asteroids it agrees with measurements for size scales from 10 cm to the largest objects of >10 km. There are no measurements of the size distribution for main-belt asteroids smaller than about 500 m, those relevant for boulder lifetimes. In Bottke et al. (2005b), the shape of the size-frequency distribution curve for those objects is the same as that of the near-earth objects. This is a consequence of the disruption law (specific energy of catastrophic disruption vs. size) used by Bottke et al. That disruption model agrees with both laboratory experiments and hydrocode calculations.

Main-belt asteroids are injected into near-earth space by drift into dynamical resonances where their orbital eccentricity is pumped up. The Yarkovsky effect (an orbit drift due to the reaction force on thermal emission, e.g., Bottke et al., 2002) is the main cause of the transfer into resonances. The ratio between Yarkovsky force and gravity is higher for smaller objects because the Yarkovsky force is (to first order) proportional to the surface area of the asteroid. Therefore the removal rate of asteroids due to Yarkovsky drift is expected to be size dependent. However, to derive the observed near-earth asteroid size-frequency distribution from the near-identical modeled distribution of small main belt asteroids, Bottke et al. (2005b) had to assume constant Yarkovsky loss for objects smaller than 1 km. A detailed model of the collisional and dynamical evolution of asteroids is beyond the scope of the present paper, but we note that a Yarkovsky drift with the expected size dependence would produce a shallower size distribution of small asteroids. That shallower size distribution in turn would increase the life time of boulders and the maximum age for large craters on asteroids. Given the accumulating evidence for "too young" craters in the asteroid main belt, it may be worthwhile to revisit the size-frequency distribution of small main-belt asteroids and the associated evolution models.

Acknowledgments

OSIRIS was built by a consortium of the Max-Planck-Institut für Sonnensystemforschung, Katlenburg-Lindau, Germany, CISAS—University of Padova, Italy, the Laboratoire d'Astrophysique de Marseille, France, the Instituto de Astrofísica de Andalucia, CSIC, Granada, Spain, the Research and Scientific Support Department of the European Space Agency, Noordwijk, The Netherlands, the Instituto Nacional de Técnica Aeroespacial, Madrid, Spain, the Universidad Politéchnica de Madrid, Spain, the Department of Physics and Astronomy of Uppsala University, Sweden, and the Institut für Datentechnik und Kommunikationsnetze der Technischen Universität Braunschweig, Germany.

The support of the national funding agencies of Germany (DLR), France (CNES), Italy (ASI), Spain (MEC), Sweden (SNSB), and the ESA Technical Directorate is gratefully acknowledged.

This research has made use of NASA's Astrophysical Data System.

References

Belskaya, I.N., Fornasier, S., Krugly, Y.N., Shevchenko, V.G., Gaftonyuk, N.M., Barucci, M.A., Fulchignoni, M., Gil-Hutton, R., 2010. Puzzling asteroid 21 Lutetia: our knowledge prior to the Rosetta fly-by. Astron. Astrophys. 515, A29.

Benz, W., Asphaug, E., 1999. Catastrophic Disruptions Revisited. Icarus 142, 5–20.

Bertini, I., Sabolo, W., Gutiérrez, P.J., Marzari, F., Snodgrass, C., Tubiana, C., Moissl, R., Pajola, M., Lowry, S.C., Barbieri, C., Ferri, F., Davidsson, B., Sierks, H., the OSIRIS team., 2012. Search for satellites near(21) Lutetia using OSIRIS/Rosetta images. Planetary and Space Science 66, 64–70.

Bottke, W.F., Vokrouhlický, D., Rubincam, D., Brož, M., 2002. Dynamical evolution of asteroids and meteoroids using the Yarkovsky effect. In: Bottke, W.F., Cellino, A., Paolicchi, P., Binzel, R.P. (Eds.), Asteorids III. Univ. of Arizona Press, Tucson, pp. 395–408.

Bottke Jr., W.F., Durda, D.D., Nesvorný, D., Jedicke, R., Morbidelli, A., Vokrouhlický, D., Levison, H., 2005a. The fossilized size distribution of the main asteroid belt. Icarus 175, 111–140.

Bottke, W.F. Jr., Durda, D.D., Nesvorný, D. Jedicke, R., Morbidelli, A., Vokrouhlický, D., Levison, H., 2005b. Linking the collisional history of the main asteroid belt to its dynamical excitation and depletion. Icarus 179, 63–94.

Carry, B., Kaasalainen, M., Leyrat, C., Merline, W.J., Drummond, J.D., Conrad, A., Weaver, H.A., Tamblyn, P.M., Chapman, C.R., Dumas, C., Colas, F., Christou, J.C., Dotto, E., Perna, D., Fornasier, S., Bernasconi, L., Behrend, R., Vachier, F., Kryszczynska, A., Polinska, M., Fulchignoni, M., Roy, R., Naves, R., Poncy, R., Wiggins, P., 2010. Physical properties of the ESA Rosetta target asteroid (21) Lutetia II. Shape and flyby geometry. Astron. Astrophys. 523, A94.

Chapman, R.C., Merline, W.J., Thomas, P.C., Joseph, J., Cheng, A.F., Izenberg, N., 2002. Impact history of Eros: craters and boulders. Icarus 155, 104–118.

Cintala, M.J., Garvin, J.B., Wetzel, S.J., 1982. The distribution of blocks around a fresh lunar mare crater. Lunar Planet. Sci. 13, 100–101.

Dombard, A.J., Barnouin, O.S., Prockter, L.M., Thomas, P.C., 2010. Boulders and ponds on the Asteroid 433 Eros. Icarus 210, 713–721.

Fujiwara, A.J., Kawaguchi, D.K., Yeomans, D.K., Abe, M., Mukai, T., Okada, T., Saito, J., Yano, H., Yoshikawa, M., Scheeres, D.J., Barnouin-Jha, O., Cheng, A.F., Demura, H., Gaskell, R.W., Hirata, N., Ikeda, H., Kominato, T., Miyamoto, H., Nakamura, A.M., Nakamura, R., Sasaki, S., Uesugi, K., 2006. The rubble pile asteroid Itokawa as observed by Hayabusa. Sci. 312, 1330–1334.

Gladman, B.J., Davis, D.R., Neese, C., Jedicke, R., Williams, G., Kavelaars, J.J., Petit, J.-M., Scholl, H., Holman, M., Warrington, B., Esquerdo, G., Tricarico, P., 2009. On the asteroid belt's orbital and size distribution. Icarus 202, 104–118.

Grady, D.E., Kipp, M.E., 1980. Continuum modelling of explosive fracture in oil shell. Int. J. Rock Mech. Min. Sci. Geomech. Abstr. 17, 147–157.

Grieger, B., Altobelli, N., Küppers, M., Schmidt, A., Völk, S., 2011. Modelling the trajectories of centimeter to meter sized chunks in the vicinity of comet 67P/Churyumov-Gerasimenko, abstract to EPSC/DPS Conference 2011.

Hörz, F., Cintala, M., 1997. Impact experiments related to the evolution of planetary regoliths. Meteoritics Planet. Sci. 32, 179–209.

Holsapple, K.A., 1993. The scaling of impact processes in planetary sciences. Ann. Rev. Earth Planet. Sci. 21, 333–373.

Holsapple, K.A., Housen, K.R., 2007. A crater and its ejecta: an interpretation of deep impact. Icarus 187, 345–356.

Housen, K.R., Schmidt, R.M., Holsapple, K.A., 1983. Crater ejecta scaling laws: fundamental forms based on dimensional analysis. J. Geophys. Res. 88, 2485–2499.

Housen, K.R., Holsapple, K.A., 2011. Ejecta from impact craters. Icarus 211, 856–875.

Keller, H.U., Barbieri, C., Koschny, D., Lamy, P., Rickman, H., Rodrigo, R., Sierks, H., A'Hearn, M.F., Angrilli, F., Barucci, M.A., Berteaux, J.-L., Cremonese, G., Da Deppo, V., Davidsson, B., De Cecco, M., Debei, S., Fornasier, S., Fulle, M., Groussin, O., Gutierrez, P.J., Hviid, S.F., Ip, W.-H., Jorda, L., Knollenberg, J., Kramm, J.R., Kührt, E., Küppers, M., Lara, L.-M., Lazzarin, M., Lopez Moreno, J., Marazi, F., Michalik, H., Naletto, G., Sabau, L., Thomas, N., Wenzel, K.-P., Bertini, I., Besse, S., Ferri, F., Kaasalainen, M., Lowry, S., Marchi, S., Mottola, S., Sabolo, W., Schröder, S.E., Spjuth, S., Vernazza, P., 2010. E-type asteroid (2867) Steins as imaged by OSIRIS on board rosetta. Sci. 327, 190–193.

Lee, S., Veverka, J., Thomas, P.C., Helfenstein, P., Belton, M.J.S., Chapman, C.R., Greeley, R., Pappalardo, R.T., Sullivan, R., Head III, J.W., 1996. Ejecta blocks on 243 Ida and on other asteroids. Icarus 120, 87–105.

Marchi, S., Barbieri, C., Küppers, M., Marzari, F., Davidsson, B., Keller, H.U., Besse, S., Lamy, P., Mottola, S., Massironi, M., Cremonese, G., 2010. The cratering history of asteroid (2867) Steins. Planet. Space Sci. 58, 1116–1123.

Marchi, S., Massironi, M., Vincent, J.-B., Morbidelli, A., Mottola, S., Marzari, F., Küppers, M., Besse, S., Thomas, N., Barbieri, C., Naletto, G., Sierks, H., 2012. The cratering history of asteroid (21) Lutetia. Planetary and Space Science 66, 87–95.

Massironi, M., Vincent, J.-B., Morbidelli, A., Mottola, S., Marzari, F., Küppers, M., Besse, S., Thomas, N., Barbieri, C., Naletto, G., Sierks, H., 2012. Geological map and stratigraphy of asteroid 21 Lutetia. Planetary and Space Science 66, 125–136.

Michikama, T., Nakamura, A.M., Hirata, N., Gaskell, R.W., Nakamura, R., Honda, T., Honda, C., Hiroaka, K., Saito, J., Demura, H., Ishiguro, M., Miyamoto, H., 2008. Size-frequency statistics of boulders on global surface of asteroid 25143 Itokawa. Earth Planets Space 60, 13–20.

O'Keefe, J.D., Ahrens, T.J., 1987. The size distribution of fragments ejected at a given velocity from impact craters. Int. J. Impact Eng. 5, 493–499.

Sierks, H., Lamy, P., Barbieri, C., Koschny, D., Rickman, H., Rodrigo, R., A'Hearn, M.F., Angrilli, F., Barucci, M.A., Berteaux, J.-L., Bertini, I., Besse, S., Carry, B., Cremonese, G., Da Deppo, V., Davidsson, B., Debei, S., De Cecco, M., De Leon, J., Ferri, F., Fornasier, S., Fulle, M., Hviid, S.F., Gaskell, R.W., Groussin, O., Gutierrez, P., Ip, W., Jorda, L., Kaasalainen, M., Keller, H.U., Knollenberg, J., Kramm, R., Kührt, E., Küppers, M., Lara, L., Lazzarin, M., Leyrat, C., Lopez Moreno, J.J., Magrin, S., Marchi, S., Marzari, F., Massironi, M., Michalik, H., Moissl, R., Naletto, G., Preusker, F., Sabau, L., Sabolo, W., Scholten, F., Snodgrass, C., Thomas, N., Tubiana, C., Vernazza, P., Vincent, J.-B., Wenzel, K.-P., Andert, T., Pätzold, M., Weiss, B.P., 2011. Images of Asteroid 21 Lutetia: A Remnant Planetesimal from the Early Solar System. Science 334, 487–490.

Stokes, G.H., Yeomans, D.K., Bottke, W.F., Chesley, S.R., Evans, J.B., Gold, R.E., Harris, A.W., Jewitt, D., Kelso, T.S., McMillan, R.S., Spahr, T.B., Worden, S.P., 2003. Report of the Near-Earth Object Science Definition Team—A Study to Determine the Feasibility of Extending the Search for Near-Earth Objects to Smaller Limiting Diameters. NASA-OSS-Solar System Exploration Division, available on 〈http://neo.jpl.nasa.gov/neo/neoreport030825.pdf〉.

Thomas, N., Barbieri, C., Keller, H.U., Lamy, P., Rickman, H., Rodrigo, R., Sierks, H., Wenzel, K.P., Cremonese, G., Jorda, L., Küppers, M., Marchi, S., Marzari, F., Massironi, M., Preusker, F., Scholten, F., Stephan, K., Barucci, M.A., Besse, S., El-Maarry, M.R., Fornasier, S., Groussin, O., Hviid, S.F., Koschny, D., Kührt, E., Martelleto, E., Moissl, R., Snodgrass, C., Tubiana, C., Vincent, J.-B., 2012. The geomorphology of (21) Lutetia: results from the OSIRIS imaging system onboard ESA's Rosetta spacecraft. Planetary and Space Science 66, 96–124.

Thomas, P.C., 1979. Surface features of Phobos and Deimos. Icarus 4, 223–243.

Thomas, P.C., Veverka, J., Robinson, M.S., Murchie, S., 2001. Shoemaker crater as the source of most ejecta blocks on the asteroid 433 Eros. Nature 413, 394–396.

Vernazza, P., Brunetto, R., Binzel, R.P., Perron, C., Fulvio, D., Strazzulla, G., Fulchignoni, M., 2009. Plausible parent bodies for enstatite chondrites and mesosiderites: implications for Lutetia's fly-by. Icarus 202, 477–486.

Vincent, J.-B., Besse, S., Marchi, S., Sierks, H., Massironi, M., the OSIRIS team., 2012. Physical properties of craters on asteroid (21) Lutetia. Planetary and Space Science 66, 79–86.

Werner, R.A., 1994. The gravitational potential of a homogeneous polyhedron or don't cut corners. Cel. Mech. Dyn. Astron. 59, 253–278.

Yoshida, F., Nakamura, T., 2007. Subaru main belt asteroid survey (SMBAS)—size and color distributions of small main-belt asteroids. Planet. Space Sci. 55, 1113–1125.